Hindawi Publishing Corporation
International Journal of Photoenergy
Volume 2015, Article ID 861353, 8 pages
http://dx.doi.org/10.1155/2015/861353

Research Article

Optimal Design of a Secondary Optical Element for a Noncoplanar Two-Reflector Solar Concentrator

Yi-Cheng Chen and Chia-Chi You

Department of Mechanical Engineering, National Central University, Jhongli, Taoyuan 320, Taiwan

Correspondence should be addressed to Yi-Cheng Chen; ethan@ncu.edu.tw

Received 11 July 2014; Revised 19 January 2015; Accepted 8 February 2015

Academic Editor: Adel A. Ismail

Copyright © 2015 Y.-C. Chen and C.-C. You. This is an open access article distributed under the Creative Commons Attribution License, which permits unrestricted use, distribution, and reproduction in any medium, provided the original work is properly cited.

This paper presents the results of a parametric design process used to achieve an optimal secondary optical element (SOE) in a noncoplanar solar concentrator composed of two reflectors. The noncoplanar solar concentrator comprises a primary parabolic mirror (M1) and a secondary hyperbolic mirror (M2). The optical performance (i.e., acceptance angle, optical efficiency, and irradiance distribution) of concentrators with various SOEs was compared using ray-tracing simulation. The parametric design process for the SOE was divided into two phases, and an optimal SOE was obtained. The sensitivity to assembly errors of the solar concentrator when using the optimal SOE was studied and the findings are discussed.

1. Introduction

Solar photovoltaic (PV) system is becoming a promising option for sustainable electricity generation as fossil fuels are decreasing on our planet. Concentrating photovoltaic (CPV) system is an important tool to improve the efficiency and to reduce the area of solar cell. The CPV systems can concentrate a large amount of sunlight into a small III-V solar cell area by using lenses or mirrors [1–5]. The primary attraction of CPV systems includes the reduced usage of expensive semiconductor solar cell and increasing the concentration ratio.

The CPV systems usually use single or dual-axis tracking to enhance performance. For CPV system, the acceptance angle $\theta_{90\%}$ is defined as the incidence angle corresponding to 90% of the maximum optical efficiency η at normal incidence. In addition, the definition of acceptance angle $\theta_{50\%}$ is the incidence angle corresponding to 50% of the maximum optical efficiency η at normal incidence. A high optical efficiency η (>70%) and a wide acceptance angle ($\theta_{90\%} > 1^\circ$) are commonly required for a CPV system. To avoid localized hot spots on the solar cell, a secondary optical element (SOE) is typically used in front of a solar cell for a solar concentrator. An SOE also improves the acceptance angle of a solar concentrator as well as irradiance uniformity on the solar cell [1, 5–7].

The optics used to collect sun energy in solar concentrators comprise three major types: refractive (using a refractive Fresnel lens), reflective (using a reflective parabolic mirror), and two-reflector (using a parabolic primary mirror and a hyperbolic secondary mirror) [6–15]. Gordon and Feuermann explored the design of two-reflector concentrator to provide radiative transfer at the thermodynamic limit [9, 12]. Chen et al. numerically investigated a solar concentrator combining a primary paraboloidal and a secondary hyperboloidal mirror by using self-developed ray-tracing simulation tool [6, 14]. Their study obtained a high concentration ratio and optimal mirror shapes of the solar concentrator.

Figure 1(a) shows a typical two-reflector solar concentrator that consists of a primary mirror (M1), a secondary mirror (M2), a solar cell, and an SOE. The initial design parameters of the two-reflector solar concentrator were as follows: the diameter of M1 = 120 mm, the diameter of the central hole of M1 = 20 mm, and the size of the square solar cell was 5.5 mm by 5.5 mm. The geometric concentration ratio (GCR) is defined as the ratio of the entrance aperture (determined by the primary mirror diameter) and the area defined by the solar cell. The GCR was 373x in this study. The other design

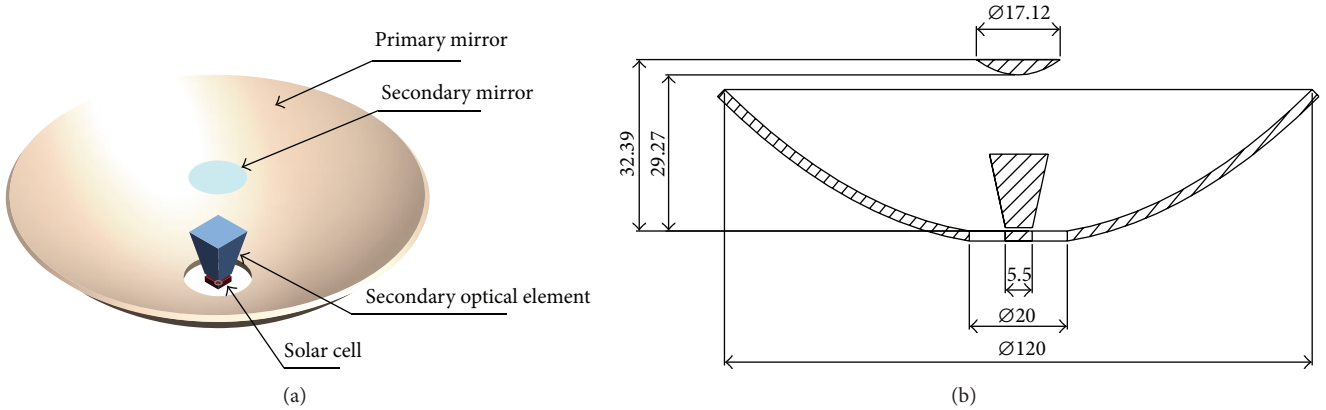

Figure 1: Illustration of the noncoplanar two-reflector solar concentrator.

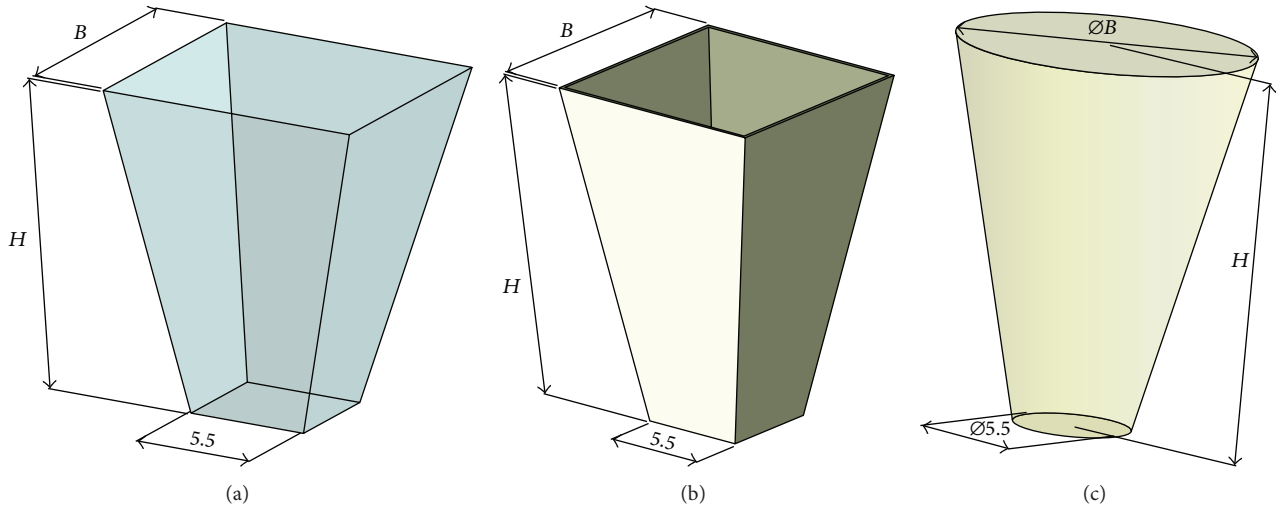

Figure 2: Three types of SOEs: (a) refractive pyramid, (b) reflective pyramid, and (c) refractive cone.

parameters of the two mirrors were preliminarily determined based on the equations proposed in [9, 12, 13]. Figure 1 illustrates the design and dimensions of the noncoplanar two-reflector concentrator with a refractive pyramid-shaped SOE. Ray-tracing simulations were performed to evaluate the optical performance, the selected two-reflector concentrator was noncoplanar (Figure 1), and the numerical aperture (NA_2) of M2 is 0.25. It is called "noncoplanar" because the rim of M1 and the backside of M2 are not in the same plane, as shown in Figure 1(b).

Based on the design of the two reflectors, ray-tracing simulation was used to predict the optical performance of the concentrator using various types of SOE. For each type of SOE, a parametric design process was performed to determine the optimal design parameters of the SOE. The SOE design process consisted of two phases, Phase I and Phase II. In Phase I, the focal point of M2 was positioned at the surface of the solar cell [15]. In Phase II, the focal point of M2 was positioned at the top surface of the SOE to improve irradiance uniformity on the cell. The predicted performance of the solar concentrator using the optimal SOE design is presented and discussed. The sensitivity of the concentrator to various misalignments of optical elements (M1, M2, and SOE) is also discussed.

2. Design Process of SOE

2.1. Phase I of SOE Design. In Phase I of the design process, the focal point of M2 was positioned on the surface of the receiver (solar cell). To increase the acceptance angle of the two-reflector solar concentrator, three types of SOEs were considered: (1) Type I: refractive pyramid-shaped SOE, (2) Type II: reflective pyramid-shaped SOE, and (3) Type III: refractive cone-shaped SOE, as depicted in Figures 2(a)–2(c), respectively. The transmittance of refractive SOE was assumed to be 96%, and the reflectance of reflective SOE was assumed to be 98%. Figures 2(a)–2(c) also depict the two major SOE design parameters, parameter B and parameter H. Parameter B represents the edge length of the top area of the two pyramid-shaped SOEs (Figures 2(a) and 2(b)) and represents the diameter of the top area of the cone-shaped SOE (Figure 2(c)). Parameter H represents the height.

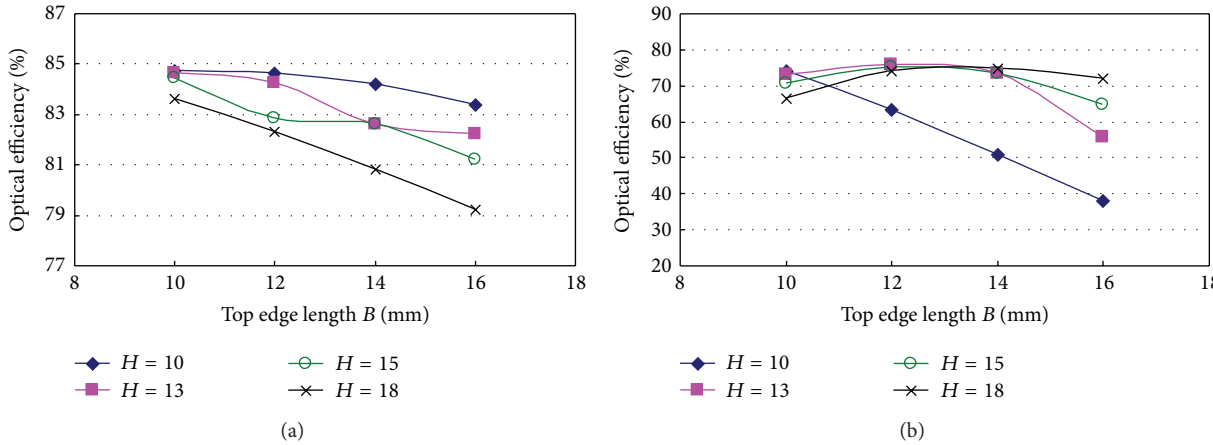

FIGURE 3: Effects of refractive pyramid SOE parameters on optical efficiency: (a) incidence angle = 0° (normal incidence) and (b) incidence angle = 1°.

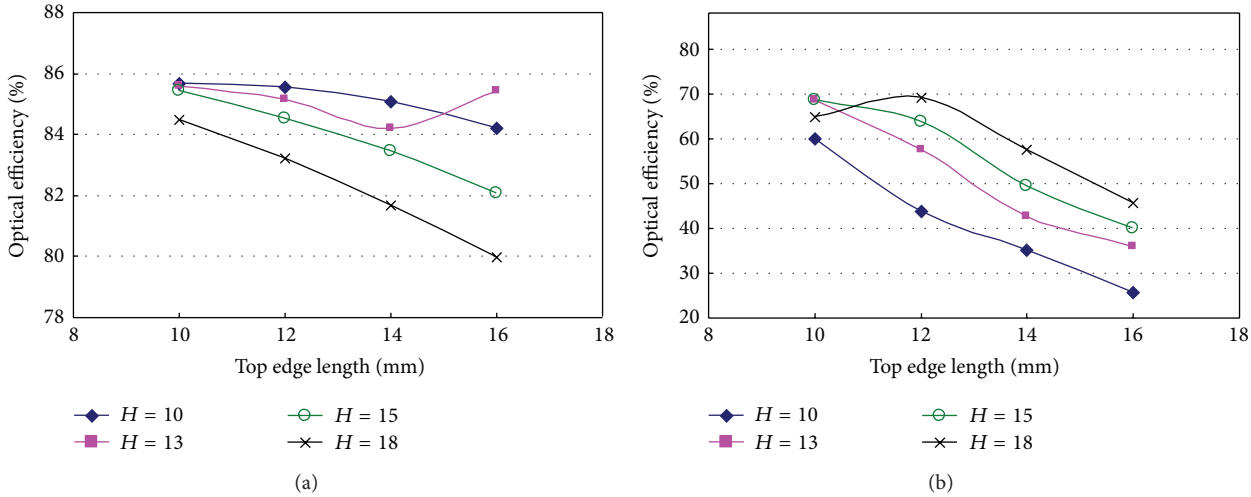

FIGURE 4: Effects of reflective pyramid SOE parameters on the optical efficiency: (a) incidence angle = 0° (normal incidence) and (b) incidence angle = 1°.

The dimensions of the bottoms of the pyramid-shaped SOEs were the same as the solar cell (5.5 mm × 5.5 mm). The diameters of the bottoms of the cone-shaped SOEs were 5.5 mm.

The effects of the design parameters H and B on the improvement of the optical efficiency of the solar concentrator were studied using ray-tracing simulation. A parametric design process was conducted using each of the three SOE types to obtain preliminary optimal SOE design parameters. The SOE designs were narrowing down to the three most promising designs, and the optical performance of the three optimal SOE designs was simulated. The results are compared and discussed.

2.1.1. SOE I: Refractive Pyramid. Figures 3(a) and 3(b) depict the effects of SOE I design parameters B (top edge length) and H (height) on the optical efficiency of the solar concentrator at incidence angles of 0° (normal incidence) and 1°, respectively. As shown in Figure 3(a), when H was fixed, optical efficiency at normal incidence decreased as B increased. Based on the simulation results shown in Figures 3(a) and 3(b), the feasible parameter sets H and B, (10, 12), (13, 12), (15, 12), and (18, 14), were selected for further investigation. The optical efficiency of the solar concentrator with SOE I of parameter set (18, 14) was good (74.9%) at incidence angle of 1°; however, the optical efficiency was only 80.8% at incidence angle of 0° (normal incidence). Therefore the parameter set (18, 14) was not selected as a feasible parameter set for SOE I.

2.1.2. SOE II: Reflective Pyramid. Figures 4(a) and 4(b) show the effects of SOE II design parameters B and H on the optical efficiency of the solar concentrator at incidence angles of 0° (normal incidence) and 1°, respectively. Figure 4(a) indicates that optical efficiency at normal incidence decreased with an increase in H or B, except when H = 13 and B = 16. However,

Table 1: Optical performance of the two-reflector solar concentrator with preliminary optimal SOEs from Phase I and Phase II.

Phase		SOE	H (mm)	B (mm)	η_{opt} (at 0°)	η_{opt} (at 1°)	$\theta_{90\%}$	$\theta_{50\%}$
I	Q1	Refractive pyramid	13	12	84.24%	75.64%	1.00	1.39
	Q2	Refractive pyramid	15	12	82.83%	75.00%	1.03	1.54
	Q3	Refractive cone	18	14	82.00%	74.82%	1.06	1.51
II	D1*	Refractive pyramid	15	10	83.52%	80.88%	1.11	1.51
	D2	Refractive cone	18	12	83.26%	78.08%	0.97	1.63

*The optimal design founded in this study.

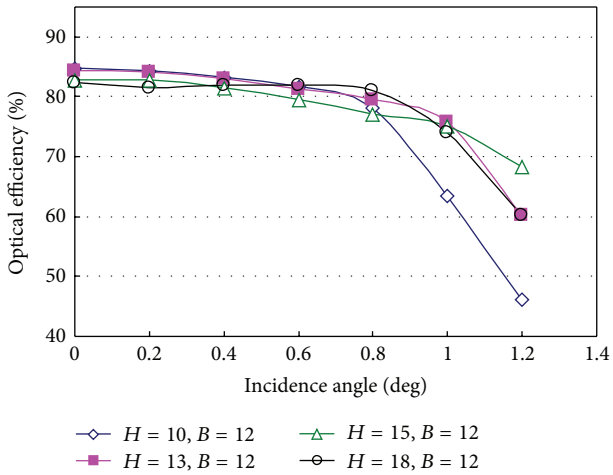

Figure 5: Optical efficiency with a refractive pyramid SOE under various incidence angles.

Figure 4(b) shows that the optical efficiency of SOE II was lower than 70% at an incidence angle of 1°. This phenomenon limits the applicability of SOE II.

2.1.3. Discussion of Pyramid-Shaped SOE. Based on a comparison of Figures 3(b) and 4(b), the refractive pyramid SOE generally exhibited higher optical efficiency than a reflective pyramid SOE at an incidence angle of 1°. This implies that using SOE I improved the acceptance angle of the concentrator more than SOE II. Consequently, the feasible parameter sets of SOE I were used to simulate the optical efficiency of the concentrator at various incidence angles; the results are depicted in Figure 5. Among the four feasible SOE I designs, two designs with the parameter sets H and B, (13, 12) and (15, 12), were preliminarily selected as optimal designs because their optical efficiencies were stable and remained higher than 60% even at an incidence angle of 1.2°.

2.1.4. SOE III: Refractive Cone. Figures 6(a) and 6(b) illustrate the effects of SOE III design parameters B (diameter of top area) and H (height) on optical efficiency at incidence angles of 0° (normal incidence) and 1°, respectively. Figure 6(a) shows that optical efficiency at normal incidence decreased as H increased. However, at an incidence angle of 1°, an increase in H resulted in increased optical efficiency (Figure 6(b)). Based on the parametric analyses of SOE III (Figure 6), feasible parameter sets H and B, (10, 12), (13, 12), (15, 12), and (18, 12), were selected for further investigation.

Figure 7 illustrates the optical efficiency of the concentrator using the four feasible designs of SOE III at various incidence angles. Among the four feasible designs of SOE III, the design with the parameter set ($H = 18$, $B = 14$) was chosen as a preliminary optimal design because of its higher optical efficiency at large incidence angles. Based on a comparison of Figures 5 and 7, the optical efficiency of concentrators using SOE III generally dropped more rapidly than that of concentrators using SOE I as the deviation of the incidence angle increased.

2.1.5. Discussion of Phase I SOE Design. The performance simulations of the two optimal designs of SOE I and one optimal design of SOE III are compared and summarized in Figure 8 and Table 1. Figure 8 shows the optical efficiency of the concentrator using the three SOEs at various incidence angles. Table 1 summarizes the design parameters of the three optimal SOE designs and the performance of the concentrator using each of the designs, including optical efficiencies at incidence angles of 0° and 1° and acceptance angles $\theta_{90\%}$ and $\theta_{50\%}$. As shown in Table 1 and Figure 8, at normal incidence, the refractive pyramid SOE design Q1 with the parameter sets H and B, (13, 12), enabled the concentrator to achieve the highest optical efficiency, 84.24%, compared with two other optimal SOE designs, Q2 (82.83%) and Q3 (82%). SOE Q3 also enabled the concentrator to achieve the highest corresponding acceptance angle $\theta_{90\%}$, 1.06°, whereas the acceptance angles $\theta_{90\%}$ for Q2 and Q1 were 1.03° and 1.00°, respectively.

The SOE designs produced in Phase I enabled the concentrator to achieve adequate acceptance angles and optical efficiencies. However, the uniformity of the irradiance distribution on the receiver was observed to be insufficient. In Phase II, the focal point of M2 was positioned at the top surface of the SOE to improve irradiance uniformity on the solar cell.

2.2. Phase II of SOE Design. In Phase II, the focal point of M2 was positioned on the top surface of the SOE to improve irradiance uniformity. Based on the results of Phase I, the preliminary optimal SOE types were observed to be the refractive pyramid and refractive cone. Consequently, Phase II considered only these two types of SOE to determine an SOE design enabling the concentrator to achieve both superior acceptance angles and irradiance uniformity.

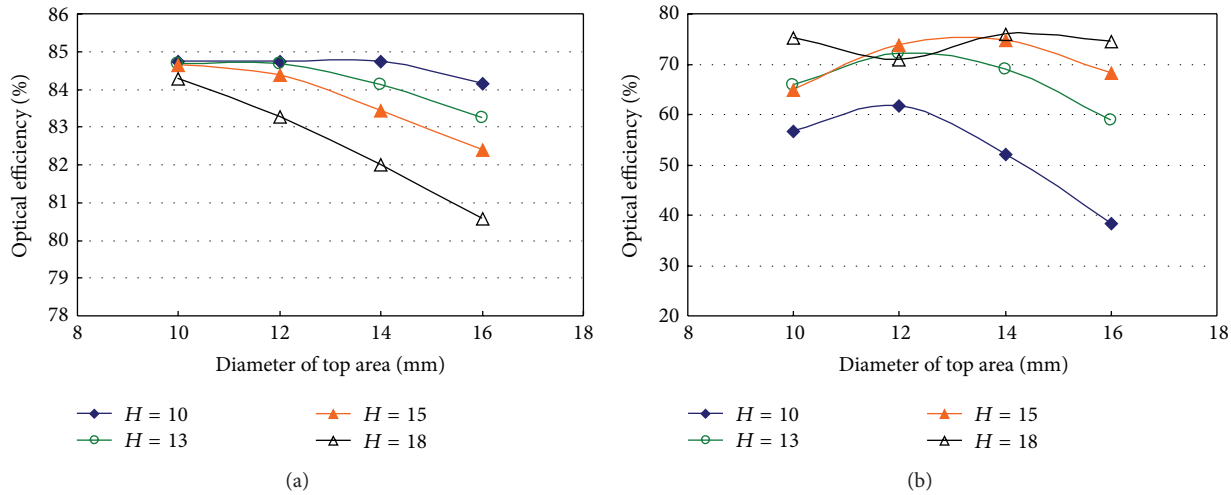

Figure 6: Effects of refractive cone SOE parameters on the optical efficiency: (a) incidence angle = 0° (normal incidence) and (b) incidence angle = 1°.

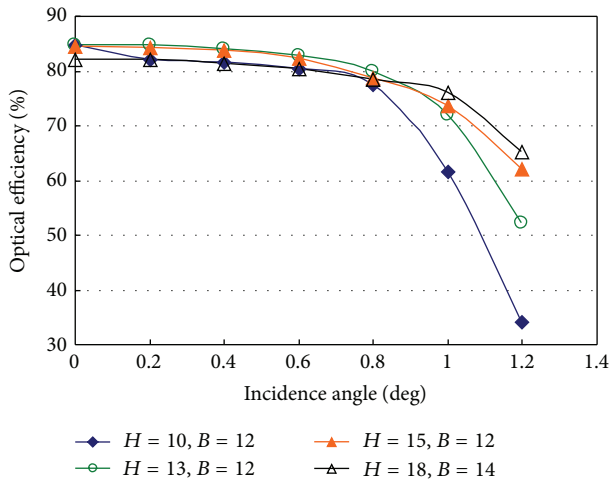

Figure 7: Optical efficiency with a refractive cone SOE under various incidence angles.

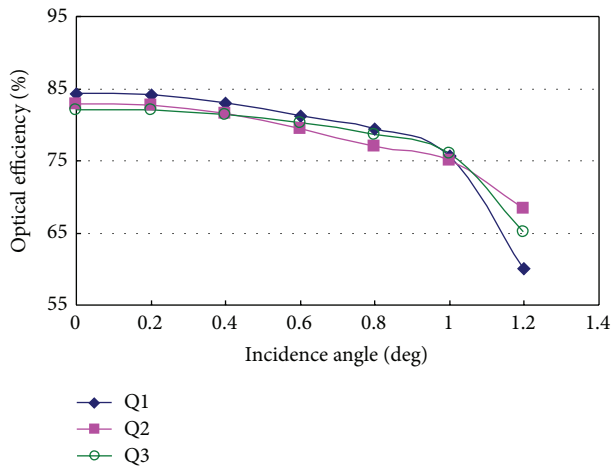

Figure 8: Optical efficiency with 3 optimal SOEs of Phase I under various incidence angles.

The two SOEs selected were (1) Type I: refractive pyramid-shaped and (2) Type II: refractive cone-shaped.

2.2.1. SOE I: Refractive Pyramid. Figures 9(a) and 9(b) illustrate the effects of SOE I design parameters B (edge length of top area) and H (height) on the optical efficiency of the concentrator at incidence angles 0° (normal incidence) and 1°, respectively. As shown in Figure 9(a), when H is fixed, optical efficiency at normal incidence decreased as B increased. Based on the simulation results shown in Figures 9(a) and 9(b), the feasible parameter sets H and B, (13, 10) and (15, 10), respectively, were selected. These feasible parameter sets exhibited the highest optical efficiency at normal incidence and incidence angle deviations.

2.2.2. SOE II: Refractive Cone. Figures 10(a) and 10(b) show the effects of the SOE III design parameters B (diameter of top area) and H (height) on optical efficiency at incidence angles 0° and 1°, respectively. Figure 10(a) shows that, at normal incidence, optical efficiency decreased when H increased. At an incidence angle of 1°, however, an increase in H resulted in increased optical efficiency, as shown in Figure 10(b). Based on the simulation results of Figure 10, the feasible parameter set H and B, (18, 12), was selected.

2.2.3. Discussion of Phase II SOE Design. Figure 11 depicts optical efficiency at various incidence angles of the two optimal SOEs selected in Phase II. Table 1 summarizes the optical performance of the solar concentrator when using these two SOEs, including optical efficiency at incidence angles 0° and 1° and acceptance angles $\theta_{90\%}$ and $\theta_{50\%}$. As shown in Table 1 and Figure 11, D1 enabled the solar concentrator to achieve a higher optical efficiency (83.52%) than D2 (83.25%) at normal

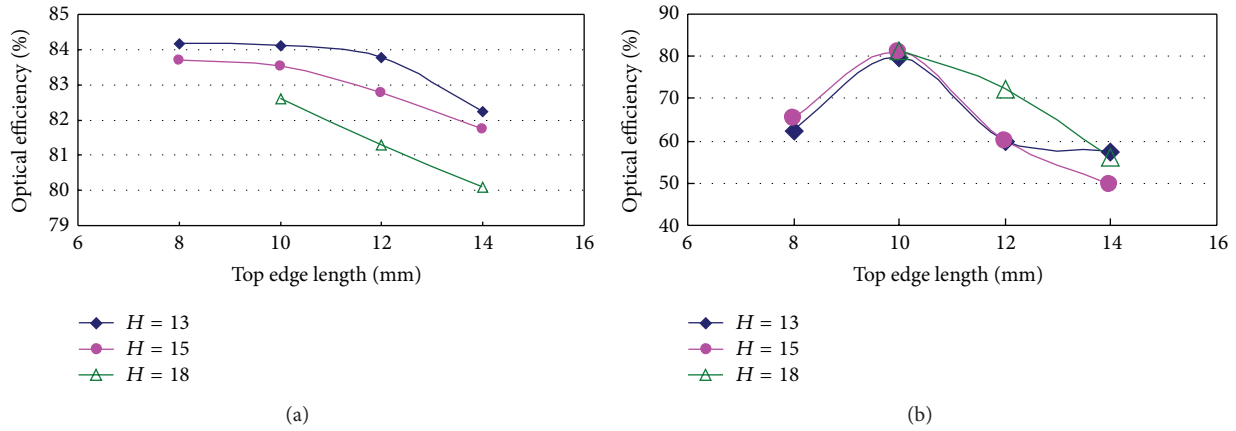

Figure 9: Effects of refractive pyramid SOE parameters (Phase II) on the optical efficiency: (a) incidence angle = 0° (normal incidence) and (b) incidence angle = 1°.

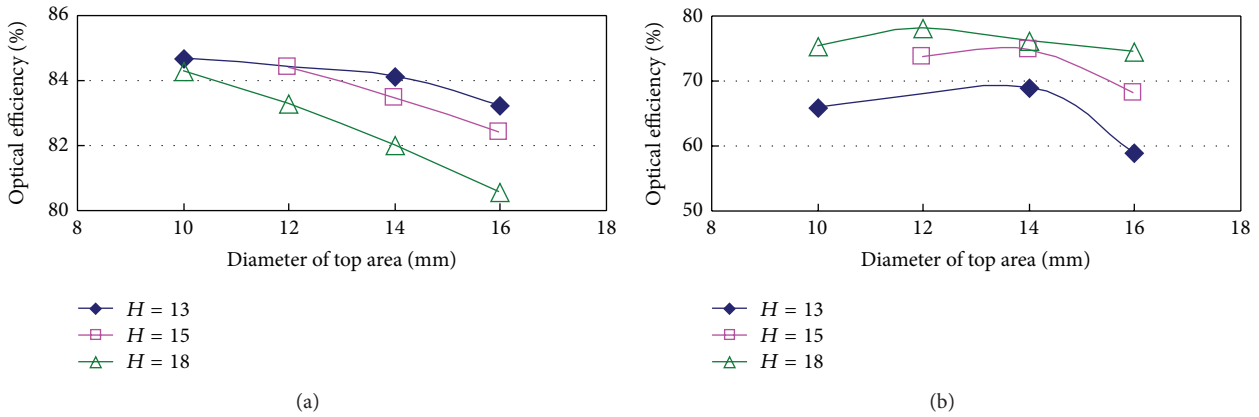

Figure 10: Effects of refractive cone SOE parameters (Phase II) on the optical efficiency: (a) incidence angle = 0° (normal incidence) and (b) incidence angle = 1°.

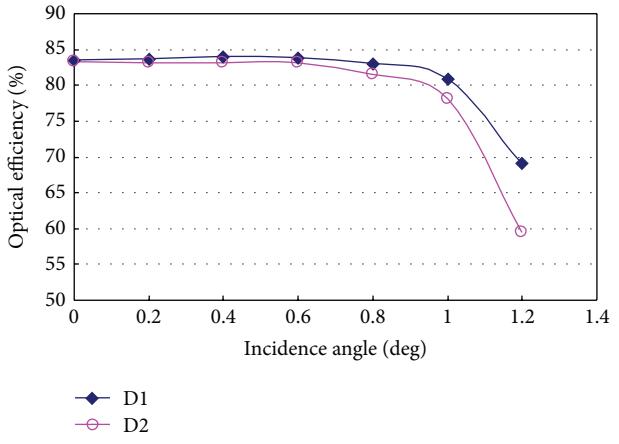

Figure 11: Optical efficiency with 2 optimal SOEs of Phase II under various incidence angles.

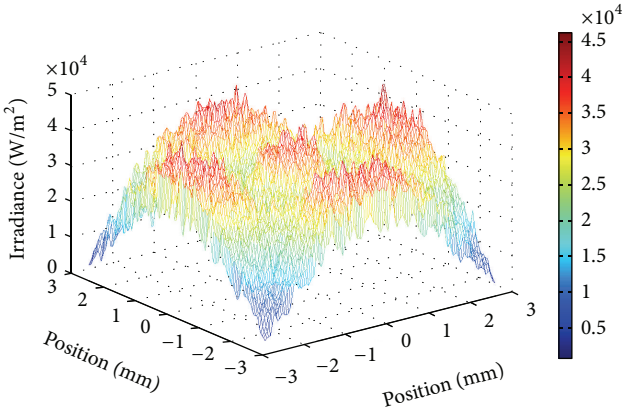

Figure 12: Irradiance distribution of the two-reflector solar concentrator with optimal SOE D1 of Phase II (normal incidence).

incidence. D1 also enabled the concentrator to achieve a higher acceptance angle $\theta_{90\%}$ (1.11°) than D2 (0.97°).

After comparing the performance results of the SOEs, it was observed that D1 yielded the optimal optical performance. The irradiance distribution of D1 on the receiver under normal incidence is shown in Figure 12; the irradiance uniformity is 67.14%.

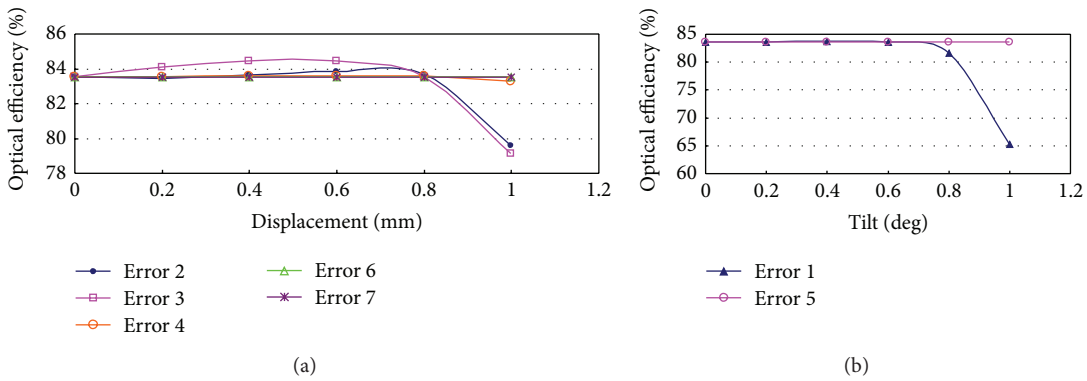

FIGURE 13: Optical efficiency under different assembly errors: (a) element displacement and (b) element tilt.

3. Sensitivity Analysis of Misalignments of Optical Elements

The effects of concentrator assembly errors on performance when using the optimal SOE, D1, were studied. The assembly errors considered included (1) tilt of M1, (2) axial displacement of M2 away from cell, (3) axial displacement of M2 toward cell, (4) radial displacement of M2, (5) tilt of M2, (6) axial displacement of cell away from M2, and (7) axial displacement of cell toward M2. Misalignments of element displacements were measured in mm, and misalignments of element tilt were measured in degrees.

Figure 13(a) shows how optical efficiency is affected by various element displacements, and Figure 13(b) shows how optical efficiency is affected by various element tilts. The displacement of M2 was the most crucial factor affecting optical efficiency, as shown in Figure 13(a). Figure 13(b) shows that optical efficiency drops dramatically if the tilt of M1 is larger than 0.8°.

Figure 14 summarizes the sensitivity of optical efficiency to the seven assembly errors. Changes in optical efficiency resulting from a 1 mm element displacement or 1° of element tilt are plotted in Figure 14. As Figure 14 shows, optical efficiency is most sensitive to M1 tilt (Error 1), displacement of M2 toward the cell (Error 3), and displacement of M2 away from the cell (Error 2) accordingly.

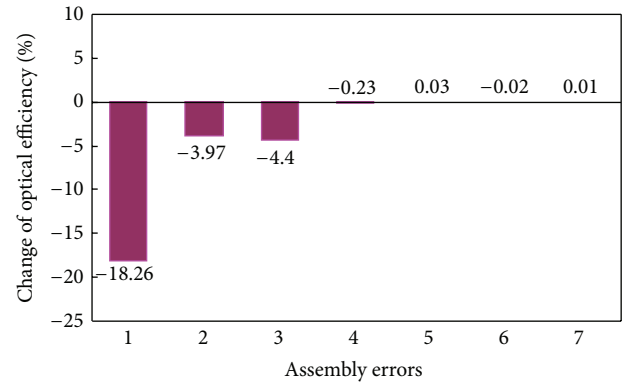

FIGURE 14: Change of optical efficiency under 7 assembly errors.

4. Conclusions

This study used a parametric design process to determine the optimal SOE for a noncoplanar, two-reflector solar concentrator. The optical performance of the solar concentrator when using several proposed SOE designs was investigated using ray-tracing simulation. Two design phases were conducted and five preliminary optimal SOE designs were selected: Q1, Q2, and Q3 from Phase I and D1 and D2 from Phase II. After comparing the optical performance of the SOE designs, D1 (refractive pyramid SOE) was selected as the optimal SOE for the noncoplanar solar concentrator. The optimal SOE, D1, enabled the concentrator to achieve a large acceptance angle ($\theta_{90\%} = 1.11^\circ$) and high optical efficiency ($\eta = 83.52\%$) at normal incidence. The sensitivity to assembly errors of the solar concentrator when using the optimal SOE was also studied, and the results indicated that the tilt of M1 was the most critical assembly error. The parametric design process presented in this study can be further applied to achieve an optimal SOE for solar concentrators with various values of GCR, NA and dimensions.

Conflict of Interests

The authors declare that there is no conflict of interests regarding the publication of this paper.

Acknowledgment

The authors would like to thank the MOST (Ministry of Science and Technology) of the Republic of China for financially supporting this research.

References

[1] A. Luque and S. Andreev, *Concentrator Photovoltaic*, Springer, Berlin, Germany, 2007.

[2] R. Winston, J. C. Miñano, and P. Benítez, *Nonimaging Optics*, Elsevier/Academic Press, New York, NY, USA, 2005.

[3] M. Khamooshi, H. Salati, F. Egelioglu, A. H. Faghiri, J. Tarabishi, and S. Babadi, "A review of solar photovoltaic concentrators,"

International Journal of Photoenergy, vol. 2014, Article ID 958521, 17 pages, 2014.

[4] R. Baños, F. Manzano-Agugliaro, F. G. Montoya, C. Gil, A. Alcayde, and J. Gómez, "Optimization methods applied to renewable and sustainable energy: a review," *Renewable & Sustainable Energy Reviews*, vol. 15, no. 4, pp. 1753–1766, 2011.

[5] B. Parida, S. Iniyan, and R. Goic, "A review of solar photovoltaic technologies," *Renewable and Sustainable Energy Reviews*, vol. 15, no. 3, pp. 1625–1636, 2011.

[6] C.-F. Chen, C.-H. Lin, and H.-T. Jan, "A solar concentrator with two reflection mirrors designed by using a ray tracing method," *Optik*, vol. 121, no. 11, pp. 1042–1051, 2010.

[7] V. M. Andreev, V. A. Grilikhes, A. A. Soluyanov, M. E. V. Vlasova, and Z. Shvarts, "Optimization of the secondary optics for photovoltaic units with Fresnel lenses," in *Proceedings of the 23th European Photovoltaic Solar Energy Conference*, pp. 126–131, 2008.

[8] M. Hernández, A. Cvetkovic, P. Benítez, and J. C. Miñano, "High-performance Köhler concentrators with uniform irradiance on solar cell," in *Nonimaging Optics and Efficient Illumination Systems V*, vol. 7059 of *Proceedings of SPIE*, San Diego, Calif, USA, August 2008.

[9] J. M. Gordon and D. Feuermann, "Tailored imaging optics for concentration and illumination at the thermodynamic limit," in *Nonimaging Optics and Efficient Illumination Systems*, vol. 5529 of *Proceedings of SPIE*, pp. 130–139, August 2004.

[10] M. McDonald, S. Home, and G. Conley, "Concentrator design to minimize LCOE," in *High and Low Concentration for Solar Electric Applications II*, vol. 6649 of *Proceedings of SPIE*, August 2007.

[11] S. Home, G. Conley, J. Gordon et al., "A solid 500 sun compound concentrator PV design," in *Proceedings of the IEEE 4th World Conference on Photovoltaic Energy Conversion*, pp. 694–697, May 2006.

[12] J. M. Gordon and D. Feuermann, "Optical performance at the thermodynamic limit with tailored imaging designs," *Applied Optics*, vol. 44, no. 12, pp. 2327–2331, 2005.

[13] N. Ostroumov, J. M. Gordon, and D. Feuermann, "Panorama of dual-mirror aplanats for maximum concentration," *Applied Optics*, vol. 48, no. 26, pp. 4926–4931, 2009.

[14] C.-F. Chen, C.-H. Lin, H.-T. Jan, and Y.-L. Yang, "Design of a solar concentrator combining paraboloidal and hyperbolic mirrors using ray tracing method," *Optics Communications*, vol. 282, no. 3, pp. 360–366, 2009.

[15] Y.-C. Chen and C.-C. You, "Design of secondary optical element for a two-reflector solar concentrator," *Applied Mechanics and Materials*, vol. 479-480, pp. 161–165, 2014.

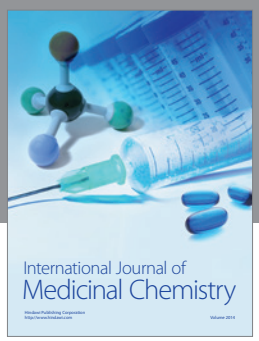

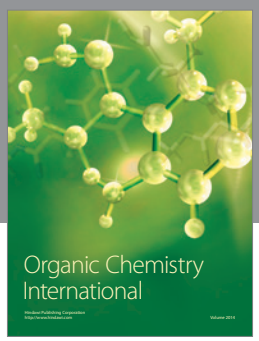

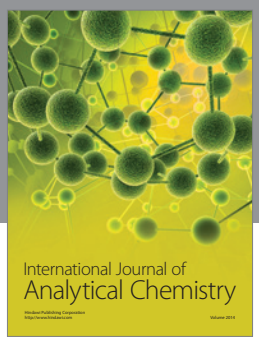

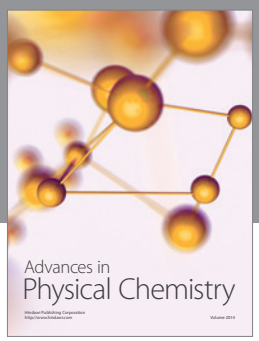

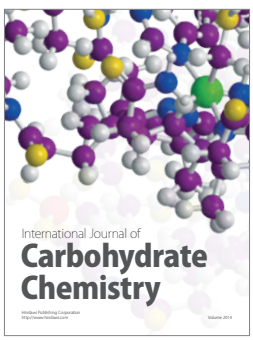

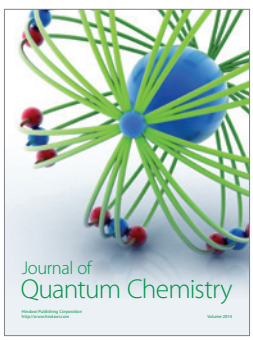

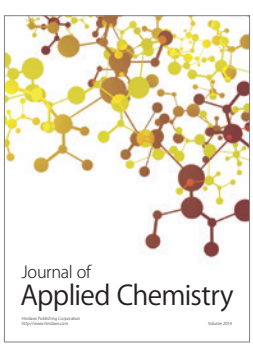

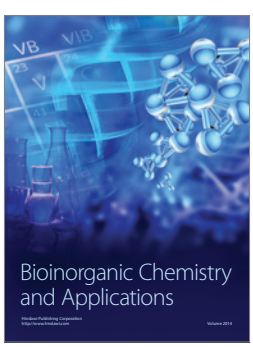

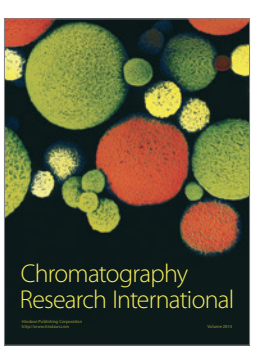

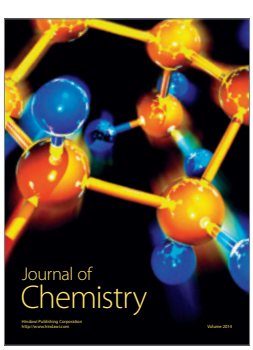

Hindawi

Submit your manuscripts at
http://www.hindawi.com